

Computational Study of Ethylene Insertion into the Metal–Hydrogen Bond of the Tetranuclear Yttrium Polyhydrido Complex $[(\eta^5\text{-C}_5\text{Me}_4\text{SiMe}_3)\text{YH}_2]_4$

Yi Luo and Zhaomin Hou*

Organometallic Chemistry Laboratory, RIKEN (The Institute of Physical and Chemical Research), and PRESTO, Japan Science and Technology Agency (JST), Hirosawa 2-1, Wako, Saitama 351-0198, Japan

Received December 7, 2006

Summary: The insertion of ethylene into a Y–H bond of the tetranuclear yttrium polyhydrido complex $(\eta^5\text{-C}_5\text{H}_4\text{SiH}_3)_4\text{Y}_4\text{H}_8$, a model of $(\eta^5\text{-C}_5\text{Me}_4\text{SiMe}_3)_4\text{Y}_4\text{H}_8$, which possesses one $\mu_4\text{-H}$, one $\mu_3\text{-H}$, and six $\mu_2\text{-H}$ atoms, was computationally investigated by the method of two-layer ONIOM (B3LYP:HF). It was found that the enthalpy barrier for the $\mu_3\text{-H}$ migratory insertion (15.3 kcal/mol) is higher than that for $\mu_2\text{-H}$ migratory insertion (10.9 kcal/mol). Both $\mu_2\text{-H}$ and $\mu_3\text{-H}$ migratory insertion reactions lead to a structurally and hence energetically identical insertion product, in which the resulting ethyl group adopts a μ_2 -bridging structure. These results suggest that the $\mu_2\text{-H}$ migratory insertion reaction pathway is kinetically preferable.

Introduction

The insertion of an alkene into a metal–hydrogen (M–H) bond (or hydrogen migratory insertion) is a key elementary step in many important catalytic and stoichiometric processes, such as hydrogenation, hydroformylation, isomerization, and polymerization.¹ In addition to mononuclear-complex-catalyzed insertion reactions, insertion processes promoted by polynuclear transition-metal and rare-earth-metal complexes have attracted considerable research interest because of the unusual reactivity contributed by the cooperation of multiple metal centers.² In this context, computational studies have mostly focused on the $\mu_1\text{-H}$ migratory insertion reaction^{3,4} but there have not been many theoretical studies on the migratory insertion of multiply

coordinated hydrogen, such as $\mu_2\text{-H}$ and $\mu_3\text{-H}$, in polynuclear complexes.⁵ During our recent studies on polynuclear rare-earth-metal polyhydrido complexes bearing cyclopentadienyl ligands,⁶ we found that they possess several unique features, structurally and chemically. For example, they not only have multiply coordinated hydrogen atoms such as $\mu_2\text{-H}$, $\mu_3\text{-H}$, and $\mu_4\text{-H}$ atoms^{6b,h} but also show high reactivity toward various unsaturated substrates, including those having unsaturated carbon–carbon bonds.^{6d} Unlike reactions with mononuclear complexes, a polynuclear complex mediated alkene insertion process, such as ethylene insertion into the Y–H bonds of the tetranuclear yttrium polyhydrido cluster $(\eta^5\text{-C}_5\text{Me}_4\text{SiMe}_3)_4\text{Y}_4\text{H}_8$ (**1**; see Figure 1),^{6h,7} may show diversity in the migratory insertion process due to its multiple metal centers and the competitive migration of multiply coordinated hydrogens. For instance, in complex **1**, the three different metal centers may have different reactivities for attack by ethylene and the migratory insertion process may involve $\mu_2\text{-H}$ or $\mu_3\text{-H}$. A computational study on such an insertion process catalyzed by polynuclear metal complexes such as **1** is of methodological importance and chemical interest. Hence, a migratory insertion of multiply coordinated hydrogen, which may be different from the $\mu_1\text{-H}$

* To whom correspondence should be addressed. Fax: (81) 48-462-4665. E-mail: hou@riken.jp (Z.H.).

(1) (a) Doherty, N. M.; Bercaw, J. E. *J. Am. Chem. Soc.* **1985**, *107*, 2670–2682. (b) Schmidt, G. F.; Brookhart, M. *J. Am. Chem. Soc.* **1985**, *107*, 1443–1444. (c) Burger, B. J.; Santarsiero, B. D.; Trimmer, M. S.; Bercaw, J. E. *J. Am. Chem. Soc.* **1988**, *110*, 3134–3146. (d) Parshall, G. W.; Ittel, S. D. *Homogeneous Catalysis*, 2nd ed.; Wiley: New York, 1992. (e) Bunel, E.; Burger, B. J.; Bercaw, J. E. *J. Am. Chem. Soc.* **1988**, *110*, 976–978. (f) Molander, G. A.; Romero, J. A. C. *Chem. Rev.* **2002**, *102*, 2161–2185. (g) Garratt, S.; Carr, A. G.; Langstein, G.; Bochmann, M. *Macromolecules* **2003**, *36*, 4276–4287.

(2) For examples, see: (a) Li, H.; Li, L.; Marks, T. J.; Sands, L. L.; Rheingold, A. L. *J. Am. Chem. Soc.* **2003**, *125*, 10788–10789. (b) Abramo, G. P.; Li, L.; Marks, T. J. *J. Am. Chem. Soc.* **2002**, *124*, 13966–13967. (c) Keaton, R. J.; Sita, L. R. *J. Am. Chem. Soc.* **2001**, *123*, 10754–10755. (d) Utiko, J.; Przybylak, S.; Jerzykiewicz, L. B.; Szafert, S.; Sobota, P. *Chem. Eur. J.* **2003**, *9*, 181–190. (e) Keaton, R. J.; Jayaratne, K. C.; Fetting, J. C.; Sita, L. R. *J. Am. Chem. Soc.* **2000**, *122*, 12909–12910. (f) Li, H.; Li, L.; Schwartz, D. J.; Metz, M. V.; Marks, T. J.; Liable-Sands, L.; Rheingold, A. L. *J. Am. Chem. Soc.* **2005**, *127*, 14756–14768. (g) Li, H.; Stern, C. L.; Marks, T. J. *Macromolecules* **2005**, *38*, 9015–9027. (h) Khoroshun, D. V.; Inagaki, A.; Suzuki, H.; Vyboishchikov, S. F.; Musaev, D. G.; Morokuma, K. *J. Am. Chem. Soc.* **2003**, *125*, 9910–9911. (i) Baar, C. R.; Jennings, M. C.; Puddephatt, R. J. *Organometallics* **2001**, *20*, 3459–3465. (j) Bigot, B.; Delbecq, F. *Organometallics* **1987**, *6*, 172–180. (k) Delbecq, F. *Organometallics* **1990**, *9*, 2223–2233. (l) Suzuki, H. *Eur. J. Inorg. Chem.* **2002**, 1009–1023. (m) Ephritikhine, M. *Chem. Rev.* **1997**, *97*, 2193–2242.

(3) For reviews, see: (a) Koga, N.; Morokuma, K. *Chem. Rev.* **1991**, *91*, 823–842. (b) Niu, S.; Hall, M. B. *Chem. Rev.* **2000**, *100*, 353–406.

(4) For examples, see: (a) Tsepis, C. A.; Kefalidis, C. E. *Organometallics* **2006**, *25*, 1696–1706. (b) Sandig, N.; Koch, W. *Organometallics* **2002**, *21*, 1861–1869. (c) Sandig, N.; Dargel, T. K.; Koch, W. *Z. Anorg. Allg. Chem.* **2000**, *626*, 392–399. (d) Ackerman, L. J.; Green, M. L. H.; Green, J. C.; Bercaw, J. E. *Organometallics* **2003**, *22*, 188–194. (e) Musaev, D. G.; Mebel, A. M.; Morokuma, K. *J. Am. Chem. Soc.* **1994**, *116*, 10693–10702. (f) Margl, P.; Deng, L.; Ziegler, T. *Organometallics* **1998**, *17*, 933–946. (g) Lauher, J. W.; Hoffmann, R. *J. Am. Chem. Soc.* **1976**, *98*, 1729–1742. (h) Sakaki, S.; Ogawa, M.; Musashi, Y.; Arai, T. *J. Am. Chem. Soc.* **1994**, *116*, 7258–7265. (i) Thorn, D.; Hoffmann, R. *J. Am. Chem. Soc.* **1978**, *100*, 2079–2090. (j) Koga, N.; Obara, S.; Kitayra, K.; Morokuma, K. *J. Am. Chem. Soc.* **1985**, *107*, 7109–7116. (k) Endo, J.; Koga, N.; Morokuma, K. *Organometallics* **1993**, *12*, 2777–2787. (l) Han, Y.; Deng, L.; Ziegler, T. *J. Am. Chem. Soc.* **1997**, *119*, 5939–5945. (m) Margl, P.; Deng, L.; Ziegler, T. *J. Am. Chem. Soc.* **1999**, *121*, 154–162.

(5) For a computational study on the reaction of a trinuclear ruthenium complex with cyclopentadiene, see: Khoroshun, D. V.; Inagaki, A.; Suzuki, H.; Vyboishchikov, S. F.; Musaev, D. G.; Morokuma, K. *J. Am. Chem. Soc.* **2003**, *125*, 9910–9911.

(6) (a) Hou, Z.; Zhang, Y.; Tardif, O.; Wakatsuki, Y. *J. Am. Chem. Soc.* **2001**, *123*, 9216–9217. (b) Tardif, O.; Nishiura, M.; Hou, Z. *Organometallics* **2003**, *22*, 1171–1173. (c) Hou, Z. *Bull. Chem. Soc. Jpn.* **2003**, *76*, 2253–2266. (d) Cui, D.; Tardif, O.; Hou, Z. *J. Am. Chem. Soc.* **2004**, *126*, 1312–1313. (e) Tardif, O.; Hashizume, D.; Hou, Z. *J. Am. Chem. Soc.* **2004**, *126*, 8080–8081. (f) Cui, D.; Nishiura, M.; Hou, Z. *Angew. Chem., Int. Ed.* **2005**, *44*, 959–962. (g) Cui, D.; Nishiura, M.; Hou, Z. *Macromolecules* **2005**, *38*, 4089–4095. (h) Luo, Y.; Baldamus, J.; Tardif, O.; Hou, Z. *Organometallics* **2005**, *24*, 4362–4366. (i) Shima, T.; Hou, Z. *J. Am. Chem. Soc.* **2006**, *128*, 8124–8125. (j) Li, X.; Baldamus, J.; Nishiura, M.; Tardif, O.; Hou, Z. *Angew. Chem., Int. Ed.* **2006**, *45*, 8184–8188.

(7) During our study on the activation of unsaturated substrates by these polynuclear polyhydrido complexes, we found that the reaction of ethylene with **1** could easily occur. However, it was difficult to isolate an ethylene insertion product because of its high activity and instability, which is one of the reasons why we computationally investigate such an insertion process.

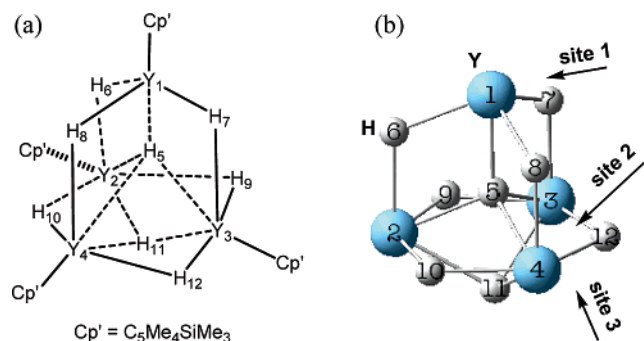


Figure 1. (a) Structure of the complex $(\eta^5\text{-C}_5\text{Me}_4\text{SiMe}_3)_4\text{Y}_4\text{H}_8$ (**1**). (b) Core part Y_4H_8 of $(\eta^5\text{-C}_5\text{H}_4\text{SiH}_3)_4\text{Y}_4\text{H}_8$, which is a model complex of **1**. The arrows indicate three possible orientations for ethylene access. Site 1 is for ethylene to approach the Y1 atom, while site 2 above the Y2Y3Y4 plane and site 3 below the Y2Y3Y4 plane are for ethylene to approach the Y4 atom.

migratory insertion process, attracted our theoretical attention. For modeling such an elementary insertion step, in this study, we have computationally investigated the insertion reaction of ethylene into the Y–H bonds of **1**.

Results and Discussion

In complex **1**, the Y1 atom bonds to four hydrogen atoms and one $\eta^5\text{-C}_5\text{Me}_4\text{SiMe}_3$ ligand, whereas each of the other three Y atoms (Y2, Y3, and Y4) bonds to five hydrogen atoms and one $\eta^5\text{-C}_5\text{Me}_4\text{SiMe}_3$ ligand, which suggests that Y1 is coordinatively unsaturated. With respect to the symmetry (C_{3v}) of the core part Y_4H_8 of $(\eta^5\text{-C}_5\text{H}_4\text{SiH}_3)_4\text{Y}_4\text{H}_8$, a model complex of **1**,⁸ there are three possible sites for ethylene access (Figure 1b). As indicated in Figure 1b, at site 1 ethylene approaches the Y1 atom, while at site 2 ethylene approaches the Y4 atom above the Y2Y3Y4 plane and at site 3 it approaches the Y4 atom below the Y2Y3Y4 plane. The $\mu_4\text{-H}$ atom was considered not to be involved in the elementary insertion step, since it is centered in the cavity of the tetrahedron constructed by the four metal atoms. The computed potential energy surface (PES) for ethylene insertion into the Y–H bonds is shown in Figure 2, in which the selected geometrical data together with the relative electronic energies (ΔE , including zero-point energy correction), enthalpies (ΔH), and free energies (ΔG , 298.15 K, 1 atm) are given. Since several small frequencies (less than 20 cm^{-1}) were computationally found for some optimized minima, the relative enthalpy (ΔH) was used for the following discussion. However, the difference between ΔH and ΔG reflects the entropy contributions. By access from site 1, complex **2** was formed with ethylene coordination to Y1. Attempts to locate a complex formed by coordination of ethylene to Y4 by access from site 2 also led to complex **2**, in which the plane of the ethylene molecule is orthogonal to the Y2Y3Y4 plane (see **2** in Figure 2). Hence, by access from site 1 or site 2 (above the Y2Y3Y4 plane), ethylene was computationally found to preferentially coordinate to the Y1 center via its carbon atoms. The access of ethylene from site 3 (below the Y2Y3Y4 plane) gave complex **4** (Figure 2). In both **2** and **4**, the interactions between the bare cluster $(\eta^5\text{-C}_5\text{H}_4\text{SiH}_3)_4\text{Y}_4\text{H}_8$ and the ethylene moiety are very weak, as suggested by the rather small binding enthalpies shown

in Figure 2 (-1.1 and -0.5 kcal/mol for **2** and **4**, respectively). In complex **4**, ethylene interacts with the bare cluster $(\eta^5\text{-C}_5\text{H}_4\text{SiH}_3)_4\text{Y}_4\text{H}_8$ through hydrogen atoms (H15 and H17) rather than the carbon atoms, even when the ethylene molecule was initially modeled parallel with the Y2Y3Y4 plane.

After the formation of complex **2**, the migratory insertion of H8 into the ethylene occurs to yield **3** by overcoming a transition state, **TS**[**2-3**], with an enthalpy barrier of 10.8 kcal/mol (path A in Figure 2). In **3**, the $\text{C13}\cdots\text{Y4}$ distance of 2.950 Å indicates an interaction between C13 and Y4. After migratory insertion of $\mu_2\text{-H8}$, the resulting CH_2CH_3 group replaced the bridging $\mu_2\text{-H8}$ to bind both Y1 (via a Y1-CH_2 bond) and Y4 (via an agostic interaction, $\text{Y4}\cdots\text{CH}_3$), while the binding modes of $\mu_4\text{-H5}$ and $\mu_3\text{-H11}$ were retained. Actually, it is computationally found that the migratory insertion reaction of $\mu_2\text{-H7}$ does also easily occur, which is equal to the $\mu_2\text{-H8}$ insertion process, due to the symmetry. It is noticed that **TS**[**2-3**] shows a five-center structure constructed by Y1, C14, H8, and Y4 atoms, in which the H8 atom not only interacts with the C13 atom but also bridges the Y1 and Y4 atoms. Such a bridging feature of H8 may stabilize the structure of **TS**[**2-3**].⁹ A similar five-center structure of a transition state was previously found in a binuclear-complex-assisted alkene insertion reaction.¹⁰ The atomic orbital interactions corroborating the cyclic five-center structure in **TS**[**2-3**] can be seen from the isosurfaces of molecular orbitals shown in Figure 3. The HOMO (Figure 3a) demonstrates the interactions of the 4d orbital of Y1 with the 1s orbital of H8 and the 2p orbital of C14. HOMO-27 and HOMO-28 (Figure 3c,d) show the orbital overlap between H8 and the ethylene moiety, and HOMO-8 (Figure 3b) shows the orbital interaction between H8(1s) and Y4(4d). Furthermore, we found that **3**, with a terminal CH_2CH_3 group ($\mu_1\text{-CH}_2\text{CH}_3$), easily goes through **TS**[**3-5'**] (with an enthalpy barrier of 7.4 kcal/mol) to give the more stable **5'** (exothermic by 3.0 kcal/mol relevant to **3**) with a CH_2CH_3 -bridging character. Analysis of the single imaginary frequency of **TS**[**3-5'**] reveals a motion of the CH_2CH_3 group to bridge Y1 and Y4 and motions of the H10 and H11 atoms toward the bond formation of Y1–H10 and bond breakage of Y3–H11, respectively, indicating that an exchange in binding mode between H10 (from μ_2 to μ_3) and H11 (from μ_3 to μ_2) is concerted with the alkyl-bridging process (see the Supporting Information for the displacement vectors associated with the imaginary frequency of **TS**[**3-5'**]). An attempt to locate a more stable minimum with a $\mu_3\text{-CH}_2\text{CH}_3$ connection led to **5'** instead, which has the $\mu_2\text{-CH}_2\text{CH}_3$ bridging character.¹¹

In comparison with complex **2**, the coordination complex **4** needs to overcome a higher enthalpy barrier (15.3 kcal/mol) to give the insertion product **5** via **TS**[**4-5**] (path B in Figure 2). One may notice that, from **4** to **TS**[**4-5**], the ethylene moiety needs to rotate about 90° around its $\text{C}=\text{C}$ bond axial with breaking of the Y4–H11 bond, which may be why the migratory insertion of $\mu_3\text{-H11}$ is kinetically unfavorable relative to that of $\mu_2\text{-H8}$. The free-energy barriers shown in Figure 2 also suggest that the $\mu_2\text{-H8}$ migratory insertion process (barrier of 12.0 kcal/mol) is more kinetically favorable than the $\mu_3\text{-H11}$ insertion reaction (barrier of 22.8 kcal/mol). IRC calculations

(9) Such a bridging feature of H8 in **TS**[**2-3**] plays an important role in the stability of the transition state, like an agostic interaction does.

(10) Luo, Y.; Hou, Z. *Organometallics* **2006**, *25*, 6162–6165.

(11) Although the product of an ethylene insertion reaction mediated by **1** could not be structurally characterized due to its instability, the reaction product of styrene with $(\eta^5\text{-C}_5\text{Me}_4\text{SiMe}_3)\text{Y}(\mu\text{-H})_2\text{Y}_4(\text{THF})$, which has been structurally characterized previously,^{5b} shows a structural feature of the benzylic phenyl group bridging two Y atoms, which is similar to the $\text{CH}_2\text{-CH}_3$ -bridging structural character in **5'**.

(8) Since the frequency calculation of the geometrically optimized $(\eta^5\text{-C}_5\text{H}_5)_4\text{Y}_4\text{H}_8$ model complex at the level of B3LYP indicates imaginary vibration modes corresponding to Cp-ring ($\eta^5\text{-C}_5\text{H}_5$) rotations, we considered that the electronic effect of substitution on a Cp ring, such as an SiMe₃ group, may play an important role in the stability of **1**. Hence, we use $(\eta^5\text{-C}_5\text{H}_4\text{SiH}_3)_4\text{Y}_4\text{H}_8$ rather than $(\eta^5\text{-C}_5\text{H}_5)_4\text{Y}_4\text{H}_8$ to model **1** in the present study.

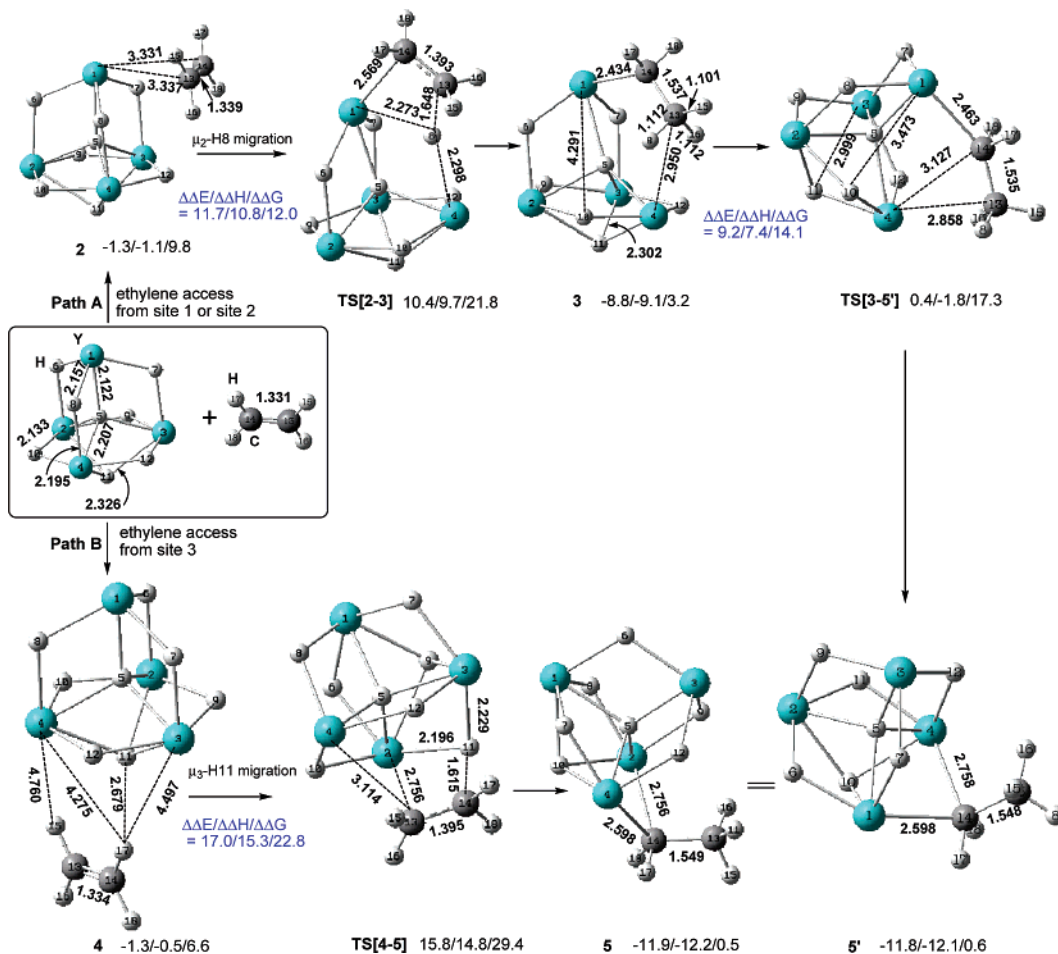


Figure 2. Computed potential energy surface. Path A is for ethylene access from site 1 or site 2, and path B is for access from site 3. Distances are given in Å, and the assignments of access sites are shown in Figure 1. Each Y atom bonds to one $\eta^5\text{-C}_5\text{H}_4\text{SiH}_3$ ligand, which is omitted for clarity. The relative electronic energy (ΔE , including zero-point energy correction), enthalpy (ΔH), and free energy (ΔG , 298.15 K, 1 atm) are relative to separate ($\eta^5\text{-C}_5\text{H}_4\text{SiH}_3$) $_4\text{Y}_4\text{H}_8$ and ethylene molecules.

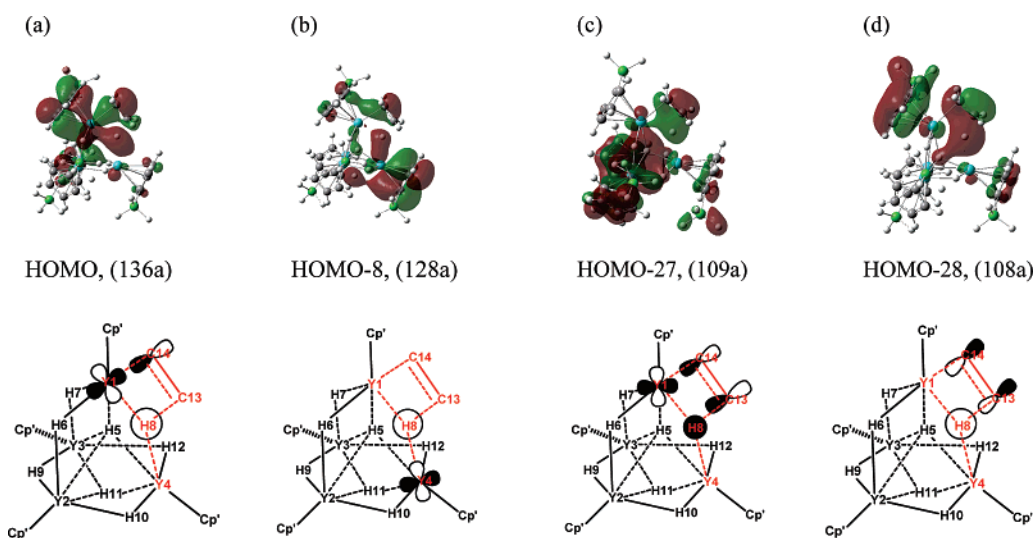


Figure 3. Molecular orbital isosurfaces of TS[2-3] showing a five-center structure constructed by Y1, C14, C13, H8, and Y4 atoms. Schematic representations (Cp' = $\eta^5\text{-C}_5\text{H}_4\text{SiH}_3$) for the atomic orbital overlaps among the five atoms (Y1, C14, C13, H8, and Y4) are shown below the corresponding molecular orbital isosurfaces.

and further geometrical releases of TS[4-5] to the minima along both sides confirmed that TS[4-5] exactly connects structures 4 and 5. For the coordination complex 4, the $\mu_2\text{-H12}$ migratory insertion product was also found, but this process was compu-

tationally found to be endothermic by 1.9 kcal/mol, possibly because of the absence of a $\mu_3\text{-H}$ atom to stabilize the structure (see the Supporting Information for the optimized structure). This suggested that the $\mu_2\text{-H12}$ migratory insertion reaction

could not thermodynamically compete with the exothermic μ_3 -H11 migratory insertion reaction. Indeed, in coordination complex **4** (Figure 2), the H12 atom is considerably further from C14 (C14...H12 distance of 5.542 Å) than is H11 (C14...H11 distance of 3.721 Å). Hence, the potential energy surface around the region of the μ_2 -H12 migratory insertion product was not further investigated.

It is also noteworthy that the insertion product **5** with an alkyl-bridging feature is exothermic by -12.2 kcal/mol relevant to the reactants, ethylene molecule, and the bare cluster (η^5 -C₅H₄-SiH₃)₄Y₄H₈ and is structurally and hence energetically equal to **5'** (relative enthalpy of -12.1 kcal/mol). That is, the migratory insertion of μ_3 -H11 and μ_2 -H8 led to the same insertion product, although insertion of μ_3 -H11 is kinetically unfavorable, implying that insertion of ethylene into a Y–H bond of (η^5 -C₅H₄-SiH₃)₄Y₄H₈ preferably follows path A in Figure 2.

In summary, a computational study of ethylene insertion into the Y–H bonds of (η^5 -C₅H₄SiH₃)₄Y₄H₈, a model of (η^5 -C₅-Me₄SiMe₃)₄Y₄H₈ with multiply coordinated hydrogen atoms, has been performed. Although the μ_2 -H and μ_3 -H migratory insertion processes are kinetically feasible and lead to identical insertion products, the μ_2 -H insertion reaction is more kinetically favorable, implying that this insertion starts with the coordination of an ethylene moiety to the coordinatively unsaturated metal center (such as Y1 in Figure 1) followed by the migratory insertion of a μ_2 -H. The resulting ethyl group easily proceeds to adopt a bridging structure, concerted with a rearrangement of metal–hydrogen bonds.

Computational Details

The model compound (η^5 -C₅H₄SiH₃)₄Y₄H₈ is used for modeling complex **1**, (η^5 -C₅Me₄SiMe₃)₄Y₄H₈. The computations were carried out with the two-layer ONIOM (B3LYP:HF) method¹² as implemented in the Gaussian03 program.¹³ In the ONIOM (B3LYP:HF) computations, the four SiH₃ groups of (η^5 -C₅H₄SiH₃)₄Y₄H₈ are placed in the outside layer treated at the HF level, and the other atoms, including those in the ethylene moiety, constitute the inner layer. Hence, for the ONIOM calculation of (η^5 -C₅H₄SiH₃)₄Y₄H₈, the “model” system is (η^5 -C₅H₅)₄Y₄H₈. The ONIOM energy of the whole system is calculated as

$$E(\text{ONIOM}) = E(\text{high level, inner layer}) + E(\text{low level, real}) - E(\text{low level, inner layer})$$

where $E(\text{high level, inner layer})$ is the energy of the inner layer calculated using the high-level method (B3LYP), $E(\text{low level, real})$ is the energy of the whole system calculated using the low-level

method (HF), and $E(\text{low level, inner layer})$ is the energy of the inner layer calculated using the low-level method. For the HF calculation, the LanL2MB basis and associated effective core potential (ECP)¹⁴ were applied. For the B3LYP calculation, the LanL2DZ basis sets and associated ECP¹⁴ were used for the Y atoms, and the eight hydrogen atoms involved in the core part Y₄H₈ were treated with the 6-31G** basis set, while the C and the remaining H atoms were treated with the 6-31G* basis set. We use the term “BS” to represent the basis sets used in the B3LYP calculation. Hence, the two-layer ONIOM method used in this study can be denoted as ONIOM (B3LYP/BS:HF/LanL2MB). Actually, the ONIOM (B3LYP:HF) calculation of (η^5 -C₅H₄SiH₃)₄Y₄H₈ in this study gave geometrical results similar to the available experimental data and computations by the method of “pure” DFT combined with larger basis sets (see Table S-1 in the Supporting Information). The geometrical variations in these methods were small (less than 0.01 Å in Y–H bond lengths and 0.06 Å in Y...Y distances) in the core part, Y₄H₈. This suggests that the two-layer method used in this study is reliable for computing the present system.¹⁵ Normal-coordinate analyses were performed to verify the geometrically optimized stationary points and to obtain the zero-point energy and thermodynamic data. For the transition-state structure, the intrinsic reaction coordinate (IRC) routes in both directions toward the corresponding minima were calculated, and further geometrical releases to the minima along with both sides were performed for some TSs. The potential energy surface was described by the relative electronic energy (ΔE), including zero-point energy correction and enthalpy (ΔH). Although there are several small frequency values (less than 20 cm⁻¹) of some optimized minima, the relative free energies (ΔG , 298.15 K, 1 atm) are also given for comparison. The stabilities of the wavefunctions were tested. A C₁ symmetry point group was used throughout all calculations, and no higher molecular symmetry restriction was imposed.

Acknowledgment. This work was partly supported by a Grant-in-Aid for Scientific Research on Priority Areas (No. 18065020, “Chemistry of Concerto Catalysis”) (to Z.H.) and for Young Scientists (No. 17750061) (to Y.L.) from the Ministry of Education, Culture, Sports, Science and Technology of Japan. We thank the RIKEN Super Combined Cluster (RSCC) for computational resources.

Supporting Information Available: Text giving the full citation of ref 13 and figures and tables giving the structure of the H12 migratory insertion product, IRC results, displacement vectors associated with the imaginary frequency of all computed transition states, and optimized Cartesian coordinates and energies together with the imaginary frequencies of TSs. This material is available free of charge via the Internet at <http://pubs.acs.org>.

OM061111V

(12) (a) Svensson, M.; Humbel, S.; Froese, R. D. J.; Matsubara, T.; Sieber, S.; Morokuma, K. *J. Phys. Chem.* **1996**, *100*, 19357–19363. (b) Maseras, F.; Morokuma, K. *J. Comput. Chem.* **1995**, *16*, 1170–1179. (c) Vreven, T.; Morokuma, K. *J. Comput. Chem.* **2000**, *21*, 1419–1432.

(13) Frisch, M. J.; et al. *Gaussian 03*, Revision C.01; Gaussian, Inc., Wallingford, CT, 2004. See the Supporting Information for a full citation.

(14) (a) Hay, P. J.; Wadt, W. R. *J. Chem. Phys.* **1985**, *82*, 270–283. (b) Wadt, W. R.; Hay, P. J. *J. Chem. Phys.* **1985**, *82*, 284–298. (c) Hay, P. J.; Wadt, W. R. *J. Chem. Phys.* **1985**, *82*, 299–310.

(15) In view of this point, we chose the two-layer ONIOM (B3LYP:HF) method for the larger system, (η^5 -C₅H₄SiH₃)₄Y₄H₈ + C₂H₄, in order to reduce computational demands.